

Constructing topological models by symmetrization: A projected entangled pair states study

Carlos Fernández-González,¹ Roger S. K. Mong,² Olivier Landon-Cardinal,³ David Pérez-García,^{4,5} and Norbert Schuch⁶

¹*Departamento de Física Interdisciplinar, Universidad Nacional de Educación a Distancia (UNED), 28040 Madrid, Spain*

²*Department of Physics and Astronomy, University of Pittsburgh, Pittsburgh, Pennsylvania 15260, USA*

³*Department of Physics, McGill University, Montréal, Québec, Canada H3A 2T8*

⁴*Departamento de Análisis Matemático & IMI, Universidad Complutense de Madrid, 28040 Madrid, Spain*

⁵*ICMAT, C/ Nicolás Cabrera, Campus de Cantoblanco, 28049 Madrid, Spain*

⁶*Max-Planck-Institute of Quantum Optics, Hans-Kopfermann-Strasse 1, D-85748 Garching, Germany*

(Received 10 August 2016; published 5 October 2016)

Symmetrization of topologically ordered wave functions is a powerful method for constructing new topological models. Here we study wave functions obtained by symmetrizing quantum double models of a group G in the projected entangled pair states (PEPS) formalism. We show that symmetrization naturally gives rise to a larger symmetry group \tilde{G} which is always non-Abelian. We prove that by symmetrizing on sufficiently large blocks, one can always construct wave functions in the same phase as the double model of \tilde{G} . In order to understand the effect of symmetrization on smaller patches, we carry out numerical studies for the toric code model, where we find strong evidence that symmetrizing on individual spins gives rise to a critical model which is at the phase transitions of two inequivalent toric codes, obtained by anyon condensation from the double model of \tilde{G} .

DOI: [10.1103/PhysRevB.94.155106](https://doi.org/10.1103/PhysRevB.94.155106)

I. INTRODUCTION

Topologically ordered states are exotic phases of matter which do not exhibit conventional order, but are characterized by their global entanglement pattern which leads to effects such as a topological ground space degeneracy or excitations with unconventional statistics, so-called anyons. A question of particular interest is how to construct new topologically ordered states from existing ones, with different and especially more complex topological order. One such route is anyon condensation [1–3], which removes part of the anyons from the model and generally leads to a simpler anyon theory. A different route, which has been particularly successful for fractional quantum Hall systems, is the projective construction. Here one starts from two or more copies of an initial wave function and projects them locally, such as onto singly occupied sites or onto the symmetric subspace, ideally yielding a wave function which exhibits more rich physics. This way, one can for instance construct Laughlin states from noninteracting topological insulators, or non-Abelian Read-Rezayi states from an Abelian Laughlin state [4,5]. Recently, symmetrization of multiple copies has also been applied to quantum spin systems with nonchiral topological order, such as Kitaev's toric code model or quantum doubles [6], and it has been found that such a construction can indeed give rise to wave functions with non-Abelian characteristics by starting from an Abelian model [7,8].

Projected entangled pair states (PEPS) provide a framework for the local description of entangled quantum spin systems [9], and allow us to exactly capture fixed point wave functions with nonchiral topological order such as quantum double [6,10,11] or string-net models [12–14]. In this framework, global topological order can be explained from a local symmetry in the entanglement degrees of freedom of the underlying local tensor, which codifies the capability of the model to exhibit topological order, and allows for the succinct description of its ground state manifold and topological excitations [11,15,16]. Using this description, one can efficiently check numerically

whether a model realizes the full topological model given by the underlying symmetry, or rather a simpler model obtained from it by condensation, and thus determine the topological phase of a given PEPS wave function [17–19].

In this paper we apply PEPS to study models obtained by symmetrizing topologically ordered wave functions, and to characterize their emergent topological order. Specifically, we consider models which are constructed by taking two or more copies of a quantum double $D(G)$ with underlying group G , such as the toric code, and projecting them locally onto the symmetric subspace [Fig. 1(a)]. From a Hamiltonian point of view, this requires the resulting model to be the ground state of a local symmetrized Hamiltonian, and therefore to be *locally* indistinguishable from the symmetrized $D(G)$ wave function.

We show that within the PEPS framework, symmetrizing the wave function can be understood through locally symmetrizing the corresponding tensors. This induces an additional symmetry under *locally* permuting the copies, thus giving rise to tensors with a non-Abelian symmetry group $\tilde{G} := (G \times G) \rtimes \mathbb{Z}_2$, or generalizations thereof, which provide the right algebraic structure to characterize wave functions which can locally be described as a symmetrized double $D(G)$. We analytically study the structure of the symmetrized tensor and show that if the symmetrization is carried out on sufficiently large patches [Fig. 1(b)], this always gives rise to a topological model in the same phase as $D(\tilde{G})$. In order to understand what happens when we symmetrize on smaller regions, we additionally perform numerical studies for the symmetrized toric code model $D(\mathbb{Z}_2)$, for which $\tilde{G} = D_4$, the dihedral group with eight elements, is non-Abelian. We find that the symmetrized model is in the full $D(D_4)$ phase down to symmetrizations on blocks of 2×2 plaquettes. For symmetrization on smaller blocks, we find strong evidence that the model is critical; in particular, symmetrization of single spins gives rise to a model which sits at a phase transition between two inequivalent toric code models, obtained from $D(D_4)$ by two different anyon condensations. Our work thus helps to clarify the nature of wave functions obtained

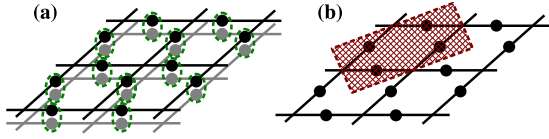


FIG. 1. (a) General setup. We take two (or more) copies of a quantum double model such as the toric code, where the spins are denoted by dots, and project the copies locally onto the symmetric subspace, indicated by the green ellipses. (b) Blocking scheme. After blocking one plaquette as indicated, we can express any double model as a G -isometric PEPS [Eq. (1)]. We also consider wave functions which are symmetrized on such blocks; we will denote the indicated block as a 1×1 block, corresponding to the symmetrized model $\text{SYM}_{1 \times 1}$.

by symmetrizing topological spin models, and demonstrates the power of PEPS to locally characterize topologically ordered wave function and assess their structure by combining analytical and numerical tools.

II. PROJECTED ENTANGLED PAIR STATES AND TOPOLOGICAL ORDER

Let us start by introducing projected entangled pair states (PEPS) and their relation to topologically ordered states. We will consider a square lattice on a torus of size $N_h \times N_v =: N$. A PEPS is constructed from a five-index tensor $A_{\alpha\beta\gamma\delta}^i$ with *physical index* $i = 1, \dots, d$ and *virtual indices* $\alpha, \dots, \delta = 1, \dots, D$, with D the *bond dimension*, depicted in Fig. 2(a). The tensors are placed on the lattice sites, and adjacent indices are contracted (i.e., identified and summed over), indicated by connected lines in Fig. 2(b). We are then left with an N -index tensor c_{i_1, \dots, i_N} which defines the PEPS wave function $|\psi\rangle = \sum c_{i_1, \dots, i_N} |i_1, \dots, i_N\rangle$.

PEPS can exactly capture topological fixed point wave functions, such as quantum double and string-net models [10,11,13,14]. In particular, for the quantum double $D(G)$ of a finite group G , the PEPS tensor A describing a block of 2×2 spins as in Fig. 1(b), i.e., one plaquette, is up to local unitaries

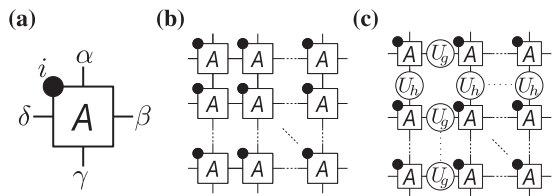


FIG. 2. Construction of PEPS. (a) Five-index tensor A with physical index i (dot) and virtual indices α, \dots, δ (lines). (b) The PEPS is constructed by forming a 2D lattice and contracting the connected virtual indices. (c) Different ground states on the torus can be parametrized by placing strings of symmetry operations U_g, U_h , with $gh = hg$, around the torus.

on the physical indices of the form

$$A = \frac{1}{|G|} \sum_{g \in G} U_g \otimes U_g^\dagger \quad (1)$$

where on the right-hand side, the legs inside the shaded area jointly describe the physical index, the $D \times D$ matrices $U_g = \sum_h |gh\rangle\langle g|$ are the regular representation of G (thus $D = |G|$), and they act from right to left and bottom to top. Differently speaking, if A is interpreted as a map \mathcal{P}_A from the virtual to the physical indices, it is of the form $\mathcal{P}_A = \frac{1}{|G|} \sum_g U_g \otimes U_g \otimes \bar{U}_g$, the projector onto the invariant subspace. As \mathcal{P}_A is an isometry on the G -invariant subspace, these PEPS are denoted as G -isometric. Note that such an A is invariant under applying U_g (or U_g^\dagger) to all virtual indices at the same time; this can in particular be used to parametrize the ground state manifold of the model's parent Hamiltonian by placing strings of U_g (U_h) along the horizontal (vertical) boundary [Fig. 2(c)], which can be freely moved (as long as $gh = hg$) due to the aforementioned condition [11].

We can modify a G -isometric tensor by adding deformations to the physical system $\mathcal{P}_{A'} = \Delta \mathcal{P}_A$; the resulting tensor is still invariant under applying U_g and thus allows for the same ground space parametrization. As long as Δ is invertible, the deformation can be “kicked back” onto the Hamiltonian, implying that the ground space degeneracy in the finite volume remains unchanged [11,20]; this might break down, however, in the thermodynamic limit [17], as we will also see later. Of particular interest later on will be the case where $\Delta = \Gamma^{\otimes 4}$ acts on all four physical subindices independently, replacing U_g by $X_g := U_g \Gamma_g$, and Γ commutes with U_g , i.e., it only changes the weight of each irrep sector.

An important observation is that the choice of U_g (or X_g) is not unique, and there are many different representations for a wave function constructed from tensors of the form Eq. (1) which are equivalent up to local unitaries. To this end, consider two adjacent sites of a PEPS constructed from such tensors,

$$\frac{1}{|G|^2} \sum_{g,h \in G} U_g \otimes U_h \otimes U_g^\dagger \otimes U_h^\dagger, \quad (2)$$

where either $U_g \equiv X_g$ or $U_g \equiv Y_g$, without any assumption on the structure of X_g and Y_g . Then, the state between the physical spins labeled A and B is of the form $|\chi_{g,h}(U)\rangle = \sum_{ij} (U_g^\dagger U_h)_{ij} |i,j\rangle$, where $U = X, Y$. However, as long as the angles between the $|\chi_{g,h}(U)\rangle$ are preserved, this is

$$\text{tr}[X_g^\dagger X_h X_{h'}^\dagger X_{g'}] = \text{tr}[Y_g^\dagger Y_h Y_{h'}^\dagger Y_{g'}], \quad (2)$$

we can always find an isometry T acting on AB which maps $T : |\chi_{g,h}(X)\rangle \mapsto |\chi_{g,h}(Y)\rangle$, and thus the corresponding

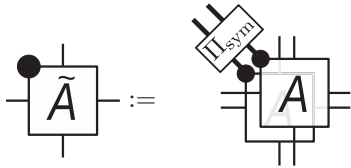
PEPS with $U_g \equiv X_g$ or $U_g \equiv Y_g$ are equivalent up to local unitaries. An important special case of this equivalence is given by the case where a unitary representation $X_g \equiv U_g = \bigoplus_{\alpha} D^{\alpha}(g) \otimes \mathbb{I}_{m_{\alpha}}$ with irreducible representations (irreps) D^{α} with multiplicity m_{α} is replaced by $Y_g \equiv \Gamma \hat{U}_g$, where $\hat{U}_g = \bigoplus D^{\alpha}(g)$ is multiplicity-free, and $\Gamma = \bigoplus m_{\alpha}^{1/4} \mathbb{I}_{d_{\alpha}}$ (with d_{α} the dimension of the irrep α) adjusts the weight of the irreps [11].

We thus see that all what matters when characterizing a U_g -invariant tensor of the form (1), with $U_g = \bigoplus_{\alpha} w_{\alpha}^{1/4} D^{\alpha}(g) \otimes \mathbb{I}_{m_{\alpha}}$, is the total weight $w_{\alpha} m_{\alpha}$ of each irrep in U_g . In particular, given a tensor (1) for which the relative weights of the irreps of U_g are sufficiently close to those in the regular representation, and thus the deformation Δ required to relate the system to the fixed point model will be sufficiently close to the identity, we can show that the gap of the parent Hamiltonian will remain open, and the system will be in the $D(G)$ phase [21], as will be discussed in more detail later on [22].

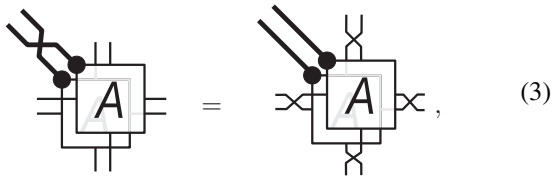
III. SYMMETRIZING TOPOLOGICAL PEPS WAVE FUNCTIONS

A. Invariance of symmetrized wave functions

Let us now consider what happens when we take two copies of a topological PEPS with symmetry group G and project them onto the symmetric subspace on the physical system,



with Π_{sym} the projection onto the symmetric subspace. It is clear that the resulting PEPS will have a virtual $G \times G$ symmetry, obtained from the independent action $U_g \otimes U_h$ of the original symmetry on the two copies. However, there is also another symmetry emerging: Since the symmetric subspace is invariant under swapping the physical indices of the two tensors, and the latter is equivalent to swapping the virtual indices between the copies,



we have that the symmetrized tensor is in addition invariant under the “flip” \mathbb{F} which swaps the virtual spaces $(U_g \otimes U_h) \mathbb{F} = \mathbb{F}(U_h \otimes U_g)$. The overall symmetry group is thus $\tilde{G} := (G \times G) \rtimes \mathbb{Z}_2$ which is generated by the elements of the direct product $(g, h) \in G \times G$, together with the semidirect action $\mathbb{F}(g, h)\mathbb{F} = (h, g)$ of the nontrivial element $\mathbb{F} \in \mathbb{Z}_2$; in particular, \tilde{G} is non-Abelian also for Abelian G . It is thus possible that the resulting symmetrized wave function has topological order described by the non-Abelian model $D(\tilde{G})$. The corresponding ground states would then be again of the form of Fig. 2(c), with U_g a representation of \tilde{G} , and are therefore obtained by either symmetrizing two copies of the original

ground states, or by additionally inserting an \mathbb{F} at either boundary which twists the two copies, i.e., by wrapping one $D(G)$ model twice around the torus and symmetrizing (cf. Ref. [23]).

Let us study the tensor obtained by symmetrizing more closely. We have $\Pi_{\text{sym}} = \frac{1}{2}(\mathbb{I} + \mathbb{F})$, and for tensors expressed as in Eq. (1), $\mathbb{F} \equiv \mathbb{F}^{\otimes 4}$ factorizes over the four physical indices. By combining the sum over U_g and U_h in the two copies of A with the sum over $\{\mathbb{I}, \mathbb{F}\}$ in $\Pi_{\text{sym}} = \frac{1}{2}(\mathbb{I}^{\otimes 4} + \mathbb{F}^{\otimes 4})$, we thus find that the symmetrized PEPS tensor \tilde{A} is of the form

$$\tilde{A} = \frac{1}{|\tilde{G}|} \sum_{k \in \tilde{G}} W_k \quad (4)$$

where

$$W_k := U_g \otimes U_h \quad \text{for } k = (g, h) \in \tilde{G},$$

$$W_k := (U_g \otimes U_h) \mathbb{F} \quad \text{for } k = (g, h) \mathbb{F} \in \tilde{G}$$

forms a unitary representation of \tilde{G} . Note that the fact that W_k is a unitary representation immediately implies that $\mathcal{P}_{\tilde{A}}$ is a projector.

B. Representation structure of symmetrized tensor

Let us now study the model obtained by symmetrizing more closely. We will in the following restrict ourselves to the case of an Abelian group G , since in this case, symmetrizing holds the promise to transform an Abelian model into a non-Abelian one; for the general case, cf. Appendix A. In order to see whether the symmetrized tensor \tilde{A} describes a topological model related to $D(\tilde{G})$, we need to study the irrep structure of W_k : if the relative weights of the different irreps are sufficiently close to the weights in the regular representation of \tilde{G} , this implies that the model is in the same phase.

We start by splitting the regular representation U_g into its one-dimensional (1D) irreps, $U_g = \bigoplus_{\alpha=1}^n D^{\alpha}(g)$, where each D^{α} is supported on a one-dimensional Hilbert space \mathcal{H}_{α} , $\bigoplus_{\alpha=1}^n \mathcal{H}_{\alpha} = \mathbb{C}^d$. This yields a corresponding decomposition

$$U_g \otimes U_h = \bigoplus_{\alpha, \beta=1}^n D^{\alpha}(g) \otimes D^{\beta}(h),$$

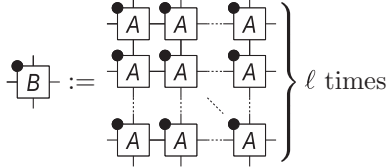
where $D^{\alpha}(g) \otimes D^{\beta}(h)$ acts on $\mathcal{H}_{\alpha} \otimes \mathcal{H}_{\beta}$; $n = |G|$ is the order of the group. We now distinguish two cases: For $\alpha = \beta$, we have that each $\mathcal{H}_{\alpha} \otimes \mathcal{H}_{\alpha}$ is invariant both under $U_g \otimes U_h$ and under \mathbb{F} , thus being a 1D irrep; as the action of $(g, 1)$ is different for each α , the irreps are all different. On the other hand, for $\alpha \neq \beta$, $\mathcal{H}_{\alpha} \otimes \mathcal{H}_{\beta} \oplus \mathcal{H}_{\beta} \otimes \mathcal{H}_{\alpha}$ is again invariant under both $U_g \otimes U_h$ and \mathbb{F} , and since $U_g \otimes U_h$ and \mathbb{F} have different eigenbases, this is a 2D irrep. There are at most $\frac{n(n-1)}{2}$ such irreps.

In order to check whether we have obtained all irreps, we can now use the counting formula for the number of irreps, $\sum d_{\alpha}^2 = |\tilde{G}|$. From the preceding arguments, we find that for the irreps we found $\sum' d_{\alpha}^2 \leq n \cdot 1^2 + \frac{n(n-1)}{2} \cdot 2^2 = 2n^2 - n$, while $|\tilde{G}| = 2n^2$. We thus see that W_k for the symmetrized wave function is even missing some irreps, and we therefore

do not expect the resulting wave function to be the phase of the double model $D(\tilde{G})$.

C. Blocking and symmetrization

The reason for the missing representations seems related to the fact that $\mathcal{H}_\alpha \otimes \mathcal{H}_\alpha$ is one dimensional, and thus \mathbb{F} can only act trivially on it. A way to remedy this would be to have irreps with higher multiplicities. To this end, we might try to symmetrize larger blocks of the system, which correspondingly carry larger representations. We therefore introduce a new tensor B obtained by blocking $\ell \times \ell$ tensors A ,



and subsequently take two copies of B rather than A and project them onto the symmetric subspace, yielding a tensor \tilde{B} .

Up to a local isometry on the physical system and an additional normalization factor $|G|^{-(\ell-1)}$, B is of the form Eq. (1), but with U_g replaced by $V_g = U_g^{\otimes \ell}$, as shown in Ref. [11]. Since $U_g^{\otimes \ell} \cong U_g \otimes \mathbb{I}_n^{\otimes \ell-1}$, we can decompose V_g as

$$V_g = \bigoplus_{\alpha=1}^n D^\alpha(g) \otimes \mathbb{I}_{\bar{n}},$$

where $\bar{n} := n^{\ell-1}$, and $D^\alpha(g) \otimes \mathbb{I}_{\bar{n}}$ is supported on an \bar{n} -dimensional subspace \mathcal{K}_α of $(\mathbb{C}^n)^{\otimes \ell} = \bigoplus_{\alpha=1}^n \mathcal{K}_\alpha$. As before, the symmetrized tensor \tilde{B} is of the form Eq. (4), but now with a representation $W'_{(g,h)} := V_g \otimes V_h$ and $W'_{(g,h)\mathbb{F}} := (V_g \otimes V_h)\mathbb{F}$.

Just as before, for each $\alpha = 1, \dots, n$ the subspace $\mathcal{K}_\alpha \otimes \mathcal{K}_\alpha$ is invariant both under all $V_g \otimes V_h$ and \mathbb{F} . However, we can now further decompose the corresponding subrepresentation. The subrepresentation is

$$\begin{aligned} (g,h) &\mapsto D^\alpha(g) \otimes D^\alpha(h) \otimes \mathbb{I}_{\mathcal{K}_\alpha \otimes \mathcal{K}_\alpha}, \\ (g,h)\mathbb{F} &\mapsto D^\alpha(g) \otimes D^\alpha(h) \otimes \mathbb{F}_{\mathcal{K}_\alpha \otimes \mathcal{K}_\alpha}, \end{aligned}$$

and all these matrices commute since $D^\alpha(g) \otimes D^\alpha(h)$ is a scalar, i.e., they are proportional to \mathbb{I} or \mathbb{F} . Therefore, it can be further split into different irreps by considering the eigenspaces of \mathbb{F} , namely the symmetric subspace $\mathcal{S}(\mathcal{K}_\alpha \otimes \mathcal{K}_\alpha)$ and the antisymmetric subspace $\mathcal{A}(\mathcal{K}_\alpha \otimes \mathcal{K}_\alpha)$ with eigenvalues $+1$ and -1 , respectively. On these two subspaces, we have subrepresentations

$$\begin{aligned} (g,h) &\mapsto D^\alpha(g) \otimes D^\alpha(h) \otimes \mathbb{I}_{\mathcal{S}(\mathcal{K}_\alpha \otimes \mathcal{K}_\alpha)}, \\ (g,h)\mathbb{F} &\mapsto D^\alpha(g) \otimes D^\alpha(h) \otimes \mathbb{I}_{\mathcal{S}(\mathcal{K}_\alpha \otimes \mathcal{K}_\alpha)}, \end{aligned}$$

and

$$\begin{aligned} (g,h) &\mapsto D^\alpha(g) \otimes D^\alpha(h) \otimes \mathbb{I}_{\mathcal{A}(\mathcal{K}_\alpha \otimes \mathcal{K}_\alpha)}, \\ (g,h)\mathbb{F} &\mapsto -D^\alpha(g) \otimes D^\alpha(h) \otimes \mathbb{I}_{\mathcal{A}(\mathcal{K}_\alpha \otimes \mathcal{K}_\alpha)}, \end{aligned}$$

respectively. Each of these is a 1D irrep with multiplicity $\dim \mathcal{S}(\mathcal{K}_\alpha \otimes \mathcal{K}_\alpha) = \bar{n}(\bar{n}+1)/2$ and $\dim \mathcal{A}(\mathcal{K}_\alpha \otimes \mathcal{K}_\alpha) = \bar{n}(\bar{n}-1)/2$, respectively, and there are n of each kind (one for each α). Clearly, all of these $2n$ irreps are distinct, since they act differently on $(g,1)$ and/or $(1,1)\mathbb{F}$.

Let us now turn to the subspaces $\mathcal{K}_\alpha \otimes \mathcal{K}_\beta \oplus \mathcal{K}_\beta \otimes \mathcal{K}_\alpha$ ($\alpha \neq \beta$). Each of them is again invariant under both $V_g \otimes V_h$ and \mathbb{F} . To decompose them further, consider a basis $\{e_1, \dots, e_{\bar{n}}\}$ of \mathcal{K}_α and a basis $\{e'_1, \dots, e'_{\bar{n}}\}$ of \mathcal{K}_β . For each $s, t \in \{1, \dots, \bar{n}\}$, the subspace $\text{span}\{e_s \otimes e'_t, e'_t \otimes e_s\}$ is still invariant under $V_g \otimes V_h$ and \mathbb{F} . This space corresponds to a 2D irrep, since for the corresponding subrepresentation, the elements $D^\alpha(g) \otimes D^\beta(h) \oplus D^\beta(g) \otimes D^\alpha(h)$ are diagonal in the basis $\{e_s \otimes e'_t, e'_t \otimes e_s\}$, while \mathbb{F} is diagonal in the basis $\{e_s \otimes e'_t \pm e'_t \otimes e_s\}$. We thus obtain \bar{n}^2 copies of a 2D irrep for each pair $\{\alpha, \beta\}$ with $\alpha \neq \beta$. Again, we get different irreps for each such pair since they act differently on $(g,1)$. Thus, we obtain in total $n(n-1)/2$ different 2D irreps, each with multiplicity \bar{n}^2 .

In total, we have $2n$ distinct 1D irreps and $n(n-1)/2$ distinct 2D irreps, and thus $\sum d_\alpha^2 = 2n + 4n(n-1)/2 = 2n^2 = |\tilde{G}|$. We have found that by blocking at least 2×2 sites, we obtain a symmetrized tensor \tilde{B} of the form Eq. (4), where W_k carries all irreps of \tilde{G} .

Of course, this still does not imply that the symmetrized PEPS described by \tilde{B} is in the same phase as the $D(\tilde{G})$ quantum double. However, we know that we can continuously deform \tilde{B} by acting with some Γ on each of the four physical indices in Eq. (4) which changes the weights of the irreps, in a way which allows us to continuously deform \tilde{B} to a tensor which corresponds to the fixed point wave function of the quantum double $D(\tilde{G})$. Such a smooth deformation of the tensor can be “kicked back” to a deformation of the parent Hamiltonian $H = \sum h_i$ [20] such that the h_i change continuously as well. While this clearly does not imply that the system is in the same phase, it will be so in the vicinity of the fixed point wave function, i.e., if the deformation $\Delta = \Gamma^{\otimes 4}$ is sufficiently close to the identity; in particular, one can derive bounds on the deformation [21] for which one can prove that the deformed Hamiltonian is connected to the gapped fixed point Hamiltonian through a gapped path, thereby guaranteeing that the system is in the $D(\tilde{G})$ topological phase. For the case under consideration, the relative weights $\frac{\bar{n}(\bar{n}+1)}{2} : \frac{\bar{n}(\bar{n}-1)}{2} : \bar{n}^2$ of the irreps need to be changed to $1 : 1 : 2$ (modulo normalization) for each of the four physical indices; the ratio of smallest and largest eigenvalue of Δ is thus $\rho = \frac{\bar{n}-1}{\bar{n}+1}$ (as each deformation Γ only carries the fourth root of the multiplicity, cf. Sec. II). A straightforward application of Appendix E of Ref. [21], where it is shown that a deformation of up to $\rho \geq \rho_0 \approx 0.967$ does not close the gap, yields that $\bar{n} \geq 2/(1-\rho_0) - 1 \approx 59.6$. We thus find that for a model with $|G| = n = 2$, symmetrizing over a block of size $\ell \geq 7$ gives rise to a model in the $D(\tilde{G})$ phase, while for $|G| \geq 59$, $\ell = 2$ is sufficient.

IV. NUMERICAL STUDY

As we have seen, symmetrizing a G -isometric PEPS wave function on a sufficiently large block gives a system which is in the phase of the $D(\tilde{G})$ topological model. However, what happens if we symmetrize on a smaller scale, such as on single tensors, or even on the level of a single site in the toric code?

In order to understand this question, we can study smooth interpolations between a model of interest and a point which we understand analytically. As long as the interpolation is

described by a smooth and invertible map acting on the physical index, the deformation corresponds to a smooth deformation of the corresponding parent Hamiltonian, and we can investigate whether along such an interpolation the system undergoes a phase transition. A convenient way to carry out such interpolations between tensors symmetrized on arbitrary block size is to use the fact that by local unitaries they can be transformed into a form where each irrep only appears once, but weighted with a diagonal matrix which accounts for the multiplicity of the irreps, as explained around Eq. (2), and interpolate the corresponding weights. In particular, this allows us to interpolate all the way from the fixed point wave function through a model symmetrized on a 2×2 block down to the model symmetrized on a single plaquette. Note that we can equivalently understand this as a procedure where we start from a model with a 2×2 plaquette unit cell which is locally equivalent to the RG fixed point wave function $D(\tilde{G})$, from which we interpolate to the 2×2 plaquette symmetrized wave function $\text{SYM}_{2 \times 2}$ and then all the way to a wave function $\text{SYM}_{1 \times 1}$ which is equivalent up to local unitaries to the wave function symmetrized on 1×1 blocks, cf. Fig. 1(b). (Note however that this is not the same as interpolating from a 2×2 symmetrized block to a block of 2×2 tensors each of which has been individually symmetrized.)

We have studied the corresponding interpolation for the symmetrized toric code model, with the result for the correlation length shown in Fig. 3: We find that the correlation length stays bounded throughout the interpolation and only diverges at $\text{SYM}_{1 \times 1}$, demonstrating that the system is in the full $D(\tilde{G})$ topological phase all the way until the $\text{SYM}_{1 \times 1}$ point. Note, however, that the Hamiltonian does not change continuously at $\text{SYM}_{1 \times 1}$, as irreps vanish (though one can define a continuous but gapless *uncle Hamiltonian* [24,25], and a parent Hamiltonian defined on larger patches might still be continuous), and while the results demonstrate that $\text{SYM}_{1 \times 1}$ has diverging correlations, the implications about the phase diagram should be taken with care.

We have also considered the interpolation between $\text{SYM}_{1 \times 1}$ and $\text{SYM}_{1/2 \times 1/2}$, the point where we have symmetrized the tensors on the level of individual spins in the toric code model [Fig. 1(a)], and have found strong evidence that the correlation length diverges all the way throughout the interpolation. In order to better understand the structure of the symmetrized wave functions $\text{SYM}_{1/2 \times 1/2}$ and $\text{SYM}_{1 \times 1}$, we have therefore considered a different interpolation which allows us to connect these models with known gapped phases.

Let us first consider $\text{SYM}_{1/2 \times 1/2}$, which is obtained by applying $\Pi_{\text{sym}} = \frac{1}{2}(\mathbb{I} + \mathbb{F})$ to each pair of spins in the two copies individually (with the spins in the conventional loop-gas basis for the toric code). We can now construct a one-parameter family by replacing Π_{sym} with

$$\Pi(\alpha) = |0,0\rangle\langle 0,0| + |1,1\rangle\langle 1,1| + \alpha |\psi^+\rangle\langle \psi^+|, \quad (5)$$

where $|\psi^+\rangle = \frac{1}{\sqrt{2}}(|0,1\rangle + |1,0\rangle)$. At $\alpha = 0$, the projection locks the spins in the two copies to be identical, and the resulting phase is unitarily equivalent to a single copy of the toric code, for $\alpha = \infty$, the system becomes a trivial product state, and for $\alpha = 1$, we obtain the $\text{SYM}_{1/2 \times 1/2}$ model. Figure 4(a) shows the correlation length (including

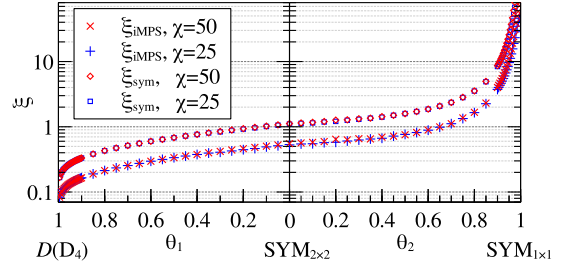


FIG. 3. Correlation length ξ for the interpolation from the fixed point $D(D_4)$ through the model symmetrized on 2×2 plaquettes ($\text{SYM}_{2 \times 2}$) to the model symmetrized on 1×1 plaquette ($\text{SYM}_{1 \times 1}$), cf. Fig. 1(b); we find that the correlation length only diverges when getting close to $\text{SYM}_{1 \times 1}$. The interpolation was realized by linearly interpolating between the irrep weights w_α of the $D(D_4)$ and $\text{SYM}_{2 \times 2}$ model and those of the $\text{SYM}_{2 \times 2}$ and $\text{SYM}_{1 \times 1}$ models, specified by the parameters θ_1 and θ_2 , respectively. We have approximated the fixed point of the transfer operator by an iMPS with bond dimensions $\chi = 25, 50$ using up to 200 iterations, and extracted the correlation length from the fixed point MPS in two ways: ξ_{iMPS} corresponds to the correlation length of the iMPS itself [i.e., $-1/\log(\lambda_2/\lambda_1)$, with $\lambda_{1,2}$ the leading eigenvectors of its transfer matrix], which captures correlations between topologically trivial excitations as well as purely electric excitations (which do not carry a string in the PEPS representation [11]). ξ_{sym} is the largest length scale set by anyon-anyon correlations with nontrivial flux (determined from the largest eigenvalue of all mixed transfer operators with a flux string $W_k \otimes \bar{W}_{k'}$ inbetween [18,19]). Here the largest length scale is given by $k \in C_4, k' \in C_1$, corresponding to the mass gap of an anyon with flux in C_4 (see Appendix B). Note that further information on the anyons could be extracted by labeling the eigenvectors by irreps.

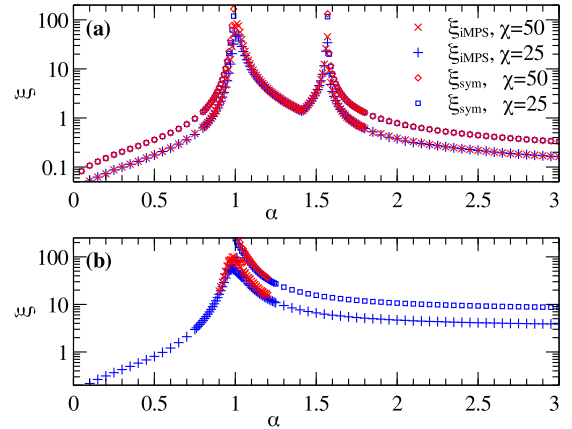


FIG. 4. (a) Correlation length for the α -interpolation [Eq. (5)] for the toric code symmetrized on a single spin; the symmetrized toric code point is at $\alpha = 1$. We find three phases: two inequivalent toric code phases for $\alpha \lesssim 1$ and $1 \lesssim \alpha \lesssim 1.57$, and a trivial phase for $\alpha \gtrsim 1.57$. (b) Corresponding interpolation for $\text{SYM}_{1 \times 1}$; we find a toric code phase on the left and a $D(D_4)$ phase on the right. Compare Fig. 3 for the numerical method and the meaning of ξ_{iMPS} and ξ_{sym} . In (a), in both the small α and large α phase, ξ_{sym} corresponds to $k = k' \in C_3$ and gives thus the confinement length of particles with flux in C_3 ; in (b), ξ_{sym} is again the mass gap of C_4 , as in Fig. 3.

correlations between pairs of anyons) along this interpolation, which gives strong indication for two phase transitions, one around $\alpha \approx 1$ and another one around $\alpha \approx 1.57$. We know that the phase on the very left is a toric code phase, and the one on the very right is a trivial phase; but what about the intermediate phase?

In order to understand this phase, we can use the parametrization of the ground space manifold of the deformed model in terms of the full symmetry W_k of the $D(\tilde{G})$ model, by placing string of symmetry actions W_k when closing the boundaries [11,17], cf. Fig. 2(c). This allows us to study the behavior of the ground states labeled by the different particle types of the $D(\tilde{G})$ model. Here we are interested in two types of information: First, what is the norm of a ground state labeled by a nontrivial anyon relative to the one labeled by the vacuum particle, and second, what is the normalization of a ground state relative to the trivial sector? Together, this allows us to understand the ground state manifold in terms of condensation of anyons: If a ground state becomes identical to the trivial ground state in the thermodynamic limit, this implies that the corresponding anyon has condensed into the ground state; and correspondingly, if the norm of a ground state is vanishing, the corresponding anyon has become confined [1,17–19].

By applying this framework, we find that the intermediate phase around $\alpha \approx 1.4$ is a toric code phase, just as the small α phase. However, we also find that the two toric code phases are obtained by condensing different particles into the vacuum, and one can therefore indeed encounter a phase transition between them. Let us note that using the same analysis, we can verify that the phase around $\alpha = 3$ is indeed the trivial phase, as for $\alpha = \infty$. Details on the method and the analysis are given in Appendix B.

We have also applied a similar analysis to $\text{SYM}_{1 \times 1}$, the model symmetrized on one plaquette, where we have replaced Π_{sym} (which now acts on four spins in the original toric code) by

$$\Pi(\alpha) = \sum_i |i, i\rangle \langle i, i| + \frac{\alpha}{2} \sum_{i>j} [|i, j\rangle + |j, i\rangle][\langle i, j| + \langle j, i|]. \quad (6)$$

Note, however, that there are two shortcomings: First, the resulting model is basis dependent. While for the single-site symmetrization, both “natural” bases for the toric code (which are related by a Hadamard transformation) give the same state, this is no longer the case. Here we have chosen the $|\pm\rangle$ basis with the tensor as in Eq. (7.5) of Ref. [11], since the dual choice gave a very large correlation length even for $\alpha = \infty$. Second, while for $\alpha = 0$, the model is again the toric code, we cannot analytically understand the structure of the model for $\alpha = \infty$, and indeed, we find that it is not a fixed point wave function and exhibits a finite correlation length $\xi \approx 3.4$. Figure 4(b) shows the result for the correlation length along the interpolation; we find that the model again undergoes a phase transition around $\alpha \approx 1$. By performing a similar analysis on the ground state as before, we find that the small α phase is a toric code phase, while the large α phase indeed realizes the $D(D_4)$ model, reconfirming that $\text{SYM}_{1/2 \times 1/2}$ is at the boundary of the $D(D_4)$ phase.

V. CONCLUSION AND DISCUSSION

We have analyzed the topological nature of wave functions obtained by symmetrizing topologically ordered states. We have shown that symmetrizing a G -isometric PEPS, corresponding to a quantum double $D(G)$, naturally gives rise to a symmetry $\tilde{G} = (G \times G) \rtimes \mathbb{Z}_2$, with \mathbb{Z}_2 acting by permuting the components in the tensor product. While this gives the resulting wave function the possibility to display $D(\tilde{G})$ topological order, it can also exhibit a simpler anyon theory obtained from $D(\tilde{G})$ by condensation. We were able to show that by symmetrizing on sufficiently large blocks, one can always ensure that the resulting model is in the $D(\tilde{G})$ phase. The effect of symmetrization on smaller patches can be analyzed numerically. For the toric code $D(\mathbb{Z}_2)$, where $\tilde{G} = D_4$, we have found that the symmetrized model remains in the full $D(D_4)$ phase down to symmetrization on 2×2 plaquettes. For symmetrization on smaller blocks, the model appears to be critical, sitting at a phase transition between inequivalent gapped topological phases.

While we performed our analysis for the case of Abelian groups G and two copies, it can immediately be generalized to the non-Abelian case and $k > 2$ copies, in which case $\tilde{G} = G^{\times k} \rtimes S_k$ (also known as the *wreath product* of G with S_k). Just as before, one can show that the multiplicities of the irreps obtained by symmetrizing k copies of $U_g^{\otimes \ell}$, with U_g the regular representation, will approach the correct ratio as ℓ grows, see Appendix A. Clearly a similar analysis can also be applied to string-net models, where the symmetry of the tensor is itself described by a matrix product operator (MPO) [15], on which we can define a semidirect action of the flip just the same way.

One might wonder what happens when we symmetrize a trivial state, $G = \{1\}$. In that case, $\tilde{G} = S_k$, which can indeed support topologically ordered states. However, since $n = |G| = 1$, it will be impossible to reach a regime where the symmetrized wave function has all irreps by blocking when starting from the regular representation of G . This can be overcome by instead starting from, e.g., a “trivial” $D = 2$ PEPS with maximally entangled bonds, with trivial group action $U_1 = \mathbb{1}_D$; just as before, symmetrizing over sufficiently large blocks (or using sufficiently large D) yields a model in the $D(S_k)$ phase (see Appendix A) which for $k \geq 3$ is again non-Abelian. While it might sound surprising that symmetrizing a product state can give rise to topological order, note that we symmetrize in a partition different from the one in which the state is a product. Also observe that since any group G can be embedded in $S_{|G|}$, this allows us to obtain any double model (such as one universal for quantum computation) by symmetrizing a product state.

An interesting perspective on symmetrized wave functions and their excitations is in terms of lattice defects in topological wave functions [26,27], and more specifically so-called genons [28]—endpoints of lattice defects in (nonsymmetrized) multi-layer systems which allow anyons to traverse between layers—which can exhibit non-Abelian statistics even for Abelian anyon models. The genons are connected by strings describing domain walls corresponding to the physical permutation symmetry Eq. (3), and are therefore confined. The projection onto the symmetric subspace gauges this symmetry, promoting it to a purely virtual symmetry on the entanglement degrees of

freedom, and thus transforms the confined lattice defects into potentially deconfined anyonic excitations [29].

ACKNOWLEDGMENTS

We acknowledge helpful conversations with A. Bernevig, A. Essin, G. Evenbly, J. Haegeman, M. Iqbal, B. Paredes, and B. Yoshida. C.F.G. acknowledges support by the Puentes Internacionales grant from Universidad Nacional de Educación a Distancia (UNED). O.L.C. is partially supported by Fonds de Recherche Quebec—Nature et Technologies and the Natural Sciences and Engineering Research Council of Canada (NSERC). D.P.G. acknowledges support from MINECO (Grant No. MTM2014-54240-P and ICMAT Severo Ochoa Project No. SEV-2015-0554) and Comunidad de Madrid (Grant QUITEMAD+CM, ref. S2013/ICE-2801), from the John Templeton Foundation through Grant No. 48322, and the European Research Council (ERC) under the European Union's Horizon 2020 research and innovation programme (Grant Agreement No. 648913). N.S. is supported by the European Research Council (ERC) under Grant No. 636201 WASCOSYS, and the Jülich-Aachen Research Alliance (JARA) through JARA-HPC Grant jara0092. Part of this work was completed at the Aspen Center for Physics, which is supported by National Science Foundation Grant No. PHY-1066293. R.S.K.M. and O.L.C. acknowledge funding provided by the Institute for Quantum Information and Matter, an NSF Physics Frontiers Center (NSF Grants No. PHY-1125565 and No. PHY-0803371) with support of the Gordon and Betty Moore Foundation (GBMF-12500028), where part of this work was carried out.

APPENDIX A: SYMMETRIZATION OF GENERAL GROUPS

In this Appendix we consider the general case in which we symmetrize k copies of a G -isometric model, and show that the resulting representation converges to multiple copies of the regular one under blocking.

Consider a finite group G with regular representation U_g , and the symmetric group S_k (or a subgroup thereof). Let $\tilde{G} := (G^{\times k}) \rtimes S_k$, where S_k acts by permuting the k -fold product $G^{\times k}$. (This is also known as the wreath product $G \wr S_k$.) Now let $V_g := U_g \otimes \mathbb{1}_{\tilde{n}}$ (where $\mathbb{1}_{\tilde{n}}$ can come either from blocking, or from adding extra entangled bonds), and consider the representation W'_g , $g \in \tilde{G}$, generated by $V_{g_1} \otimes \cdots \otimes V_{g_k}$ and the permutation action Π_g on the tensor components. The character of this representation is given by

$$\begin{aligned} \chi_{W'}(\mathbf{g}) &= \text{tr}[(V_{g_1} \otimes \cdots \otimes V_{g_k})\Pi_g] \\ &= \underbrace{\text{tr}(U_{g_1} \otimes \cdots \otimes U_{g_k})\Pi_g}_{=: \chi_W(\mathbf{g})} \underbrace{\text{tr}[(\mathbb{1}_{\tilde{n}} \otimes \cdots \otimes \mathbb{1}_{\tilde{n}})\Pi_g]}_{=: \chi_\Pi(\mathbf{g})}. \end{aligned}$$

We now have that $\chi_W(1) = |G|^k$, and $\chi_W(\mathbf{g}) = 0$ for all $\mathbf{g} \neq 1$ with trivial permutation action, $\Pi_g = \mathbb{I}$; moreover, $|\chi_W(\mathbf{g})| \leq \chi_W(1) = |G|^k$ is independent of \tilde{n} . On the other hand, $\chi_\Pi(\mathbf{g}) = \tilde{n}^c$, where c is the number of cycles in Π_g , i.e., $\chi_\Pi(\mathbf{g}) = \tilde{n}^k$ for $\Pi_g = \mathbb{I}$, and $|\chi_\Pi(\mathbf{g})| \leq \tilde{n}^{k-1}$ otherwise. We thus see that $\chi_{W'}(1) = |G|^k \tilde{n}^k$, while $|\chi_{W'}(\mathbf{g})| \leq |G|^k \tilde{n}^{k-1}$ for $\mathbf{g} \neq 1$.

Now let $\chi_\alpha(\mathbf{g})$ be the character of an irrep α of \tilde{G} , with dimension d_α . Then, the multiplicity of α in W'_g is given by

$$\begin{aligned} \mu_\alpha &= \frac{1}{|\tilde{G}|} \sum_{g \in \tilde{G}} \chi_{W'}^*(\mathbf{g}) \chi_\alpha(\mathbf{g}) \\ &= \frac{1}{|\tilde{G}|} \left[\chi_{W'}^*(1) \chi_\alpha(1) + \sum_{g \neq 1} \chi_{W'}^*(\mathbf{g}) \chi_\alpha(\mathbf{g}) \right] \\ &= \frac{1}{|\tilde{G}|} \left[|G|^k \tilde{n}^k d_\alpha + \sum_{g \neq 1} \chi_{W'}^*(\mathbf{g}) \chi_\alpha(\mathbf{g}) \right]. \end{aligned}$$

We thus have that

$$\left| \mu_\alpha - \frac{d_\alpha |G|^k \tilde{n}^k}{|\tilde{G}|} \right| = \frac{1}{|\tilde{G}|} \left| \sum_{g \neq 1} \chi_{W'}^*(\mathbf{g}) \chi_\alpha(\mathbf{g}) \right| \leq |G|^k \tilde{n}^{k-1} d_\alpha,$$

where we have used that $|\chi_\alpha(\mathbf{g})| \leq d_\alpha$. Thus, in order to obtain the correct relative weights d_α of the regular representation, the weights μ_α need to be changed by at most

$$\begin{aligned} \rho &= \frac{\min(\mu_\alpha/d_\alpha)}{\max(\mu_\alpha/d_\alpha)} = \frac{|G|^k \tilde{n}^k / |\tilde{G}| - |G|^k \tilde{n}^{k-1}}{|G|^k \tilde{n}^k / |\tilde{G}| + |G|^k \tilde{n}^{k-1}} \\ &\geq 1 - \frac{2|\tilde{G}|}{\tilde{n}}. \end{aligned}$$

As before, this yields that the symmetrized model is in the $D(\tilde{G})$ phase if $\rho \geq \rho_0 \approx 0.967$, and thus $\tilde{n} \geq 2|\tilde{G}|/(1 - \rho_0) \approx 60.6 |G|^k k!$.

APPENDIX B: IDENTIFICATION OF ANYON CONDENSATION PATTERN

In this Appendix we describe how to identify the different anyon condensations we find in the symmetrized $D(\mathbb{Z}_2)$ model.

We begin by setting a notation for the dihedral group $D_4 = (\mathbb{Z}_2 \times \mathbb{Z}_2) \rtimes \mathbb{Z}_2$, and the anyons of its quantum double. The symmetry generators of the symmetrized toric code are $X \otimes \mathbb{I}$, $\mathbb{I} \otimes X$ (for the two layers), and \mathbb{F} which flips the layers. The D_4 group has two generators $x := \mathbb{F}$ and $a := (\mathbb{I} \otimes X)\mathbb{F}$ with the group presentation $\langle x, a | x^2 = a^4 = 1, xax^{-1} = a^{-1} \rangle$. The eight group elements partition into the five conjugacy classes

$$\begin{aligned} C_1 &= \{e\}, \\ C_2 &= \{a^2\}, \\ C_3 &= \{a, a^3\}, \\ C_4 &= \{x, a^2x\}, \\ C_5 &= \{ax, a^3x\}. \end{aligned} \tag{B1}$$

Let us now consider the irreps of their normalizers $N[C]$ (defined as equivalence classes of the isomorphic normalizers $N[g] = \{h \in G : gh = hg\}$, $g \in C$) which together with C_n label the particle sectors:

(1) $N[C_1] = N[C_2] = D_4$, with irrep characters

	C_1	C_2	C_3	C_4	C_5
α_0	1	1	1	1	1
α_1	1	1	1	-1	-1
α_2	1	1	-1	1	-1
α_3	1	1	-1	-1	1
α_4	2	-2	0	0	0

(2) $N[C_3] \cong N[a] = \{e, a, a^2, a^3\} \cong \mathbb{Z}_4$ with irreps $\alpha_k(a) = i^k$.(3) $N[C_4] \cong N[x] = \{e, x, a^2, a^2x\} \cong \mathbb{Z}_2 \times \mathbb{Z}_2$ with irreps $\alpha_k(x) = (-1)^{k_1}$, $\alpha_k(a^2) = (-1)^{k_2}$, $k = 2k_2 + k_1$.(4) $N[C_5] \cong N[ax] = \{e, ax, a^2, a^3x\} \cong \mathbb{Z}_2 \times \mathbb{Z}_2$ with irreps $\alpha_k(ax) = (-1)^{k_1}$, $\alpha_k(a^2) = (-1)^{k_2}$, $k = 2k_2 + k_1$.

The irreps are given for the correspondingly listed element of the conjugacy class. Each anyon of $D(D_4)$ is labeled by one conjugacy class C_n and an irrep α_m of its normalizer. We will employ the shorthand notation nm , where $n = 1, \dots, 5$, and $m = a, b, c, \dots$ ($a \equiv 0, b \equiv 1$, etc.) to label the 22 anyons. For example, $4b$ labels the anyon with conjugacy class C_4 and irrep α_1 ; in particular, $1a$ is the trivial (vacuum) anyon. Table I lists the anyons.

On an infinitely long cylinder (or torus), there is a one-to-one correspondence between anyons and ground states; we denote these states as $|\psi_A\rangle$ where A is the anyon label. Physically, these states are constructed by starting with the wave function corresponding to the vacuum $|\psi_{1a}\rangle$, creating a pair of A - A anyons, and pulling them apart to opposite ends of the cylinder.

In order to identify the anyon condensation pattern, we compute the overlap between all possible states $|\psi_A\rangle$ in the thermodynamic limit. Several things can happen [17–19]. If *all* the states have nonvanishing norm and remain orthogonal to one another, this implies that no anyon condensation occurred and we remain in the $D(D_4)$ topological phase. However, if the norm of any state $|\psi_A\rangle$ does go to zero (relative to that of $|\psi_{1a}\rangle$), then this corresponds to the case where the anyon A has become confined, indicative of an anyon condensation process. Another possibility is that the overlap of two states $|\psi_A\rangle$ and $|\psi_B\rangle$ goes to a nonzero constant rather than being orthogonal; in such case, the anyons of the condensed theory are constructed from superpositions of A and B . In particular, an anyon C is condensed if it forms a superposition with the vacuum.

In order to numerically compute the overlap, we put $|\psi_A\rangle$ on a long cylinder (or torus) of length N_h and circumference N_v . There, a state $|\psi_A\rangle$ with $A \equiv nm$ is constructed by (i)

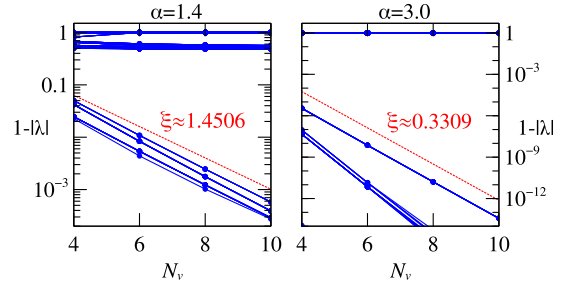


FIG. 5. Overlap per column $\lambda_{N_v} \equiv \lambda$ (on a cylinder of circumference N_v) of anyon sectors for the α -interpolation (5) of $\text{SYM}_{1/2 \times 1/2}$. One can clearly distinguish the λ which converge to 1 exponentially from those which go to a constant. For comparison, we plot $c \exp(-N_v/\xi)$, with ξ the largest correlation length of Fig. 4(a), which confirms that the overlap of ground state sectors is governed by the anyon-anyon correlations. Since there are 253 different lines, we omit labels; the condensed anyon theory extracted from the data is given in the text.

placing a string of U_g for some $g \in C_n$ along the cylinder axis when closing the boundary, and (ii) by projecting the boundary of the cylinder onto the irrep sector α_m of $N[g] \cong N[C_n]$; cf. Refs. [11,17] for details. The overlap of two states is then the overlap of the corresponding PEPS, which asymptotically scales like the N_h th power of the largest eigenvalue λ_{N_v} of one column of the corresponding mixed transfer operator, cf. Ref. [17]. We therefore need to analyze whether λ_{N_v} (normalized by the largest eigenvalue in the trivial sector) converges to one: If it does (at a sufficient rate), then $\lambda_{N_v}^{N_h} \rightarrow 1$ for a coupled limit $N_h, N_v \rightarrow \infty$, while if it does not, $\lambda_{N_v}^{N_h} \rightarrow 0$. To this end, we use exact diagonalization of the transfer operator together with finite size scaling, cf. Ref. [17].

Figure 5 shows the corresponding data for the two phases at $\alpha = 1.4$ and $\alpha = 3.0$ in the α -interpolation [Eq. (5)] of the $\text{SYM}_{1/2 \times 1/2}$ model, Fig. 4(a), and we find that we can clearly distinguish the two different scaling behaviors of λ_{N_v} . For the small α phase, we consider $\alpha = 0$, which is a fixed point wave function and thus $\lambda_{N_v} \in \{0, 1\}$ independent of N_v . We can now study the condensation and confinement of anyons as described above. For $\alpha = 0$ we find that the following ground states have nontrivial overlaps within each set: $(1a, 1c, 4a)$, $(2a, 2c, 4a)$, $(1e, 4c)$, $(2e, 4d)$, while all other wave functions have vanishing norm [30]. From this we have the anyon condensation process:

$$\begin{aligned}
 1a + 1c + 4a &\rightarrow \hat{1}, \\
 1e + 4c &\rightarrow \hat{e}, \\
 2a + 2c + 4a &\rightarrow \hat{m}, \\
 2e + 4d &\rightarrow \hat{f}.
 \end{aligned}$$

TABLE I. The anyons of $D(D_4)$ and their properties. Each anyon is its own antiparticle. The topological spin is given by $\alpha_m(g)$, where g is the representative of the conjugacy class C_n used to define the irrep characters α_m of $N[g] \cong N[C]$.

Label	1a	1b	1c	1d	1e	2a	2b	2c	2d	2e	3a	3b	3c	3d	4a	4b	4c	4d	5a	5b	5c	5d
Quantum dimension	1	1	1	1	2	1	1	1	1	2	2	2	2	2	2	2	2	2	2	2	2	2
Topological spin	1	1	1	1	1	1	1	1	1	-1	1	i	-1	-i	1	-1	1	-1	1	-1	1	-1

Indeed, the resulting phase has toric code topological order: The anyons $\hat{1}$, \hat{e} , and \hat{m} are bosons (i.e., their components have topological spin $+1$), while \hat{f} is a fermion (with topological spin -1). The mutual statistics of \hat{e} , \hat{m} , and \hat{f} are fermionic (i.e., their mutual S -matrix elements are -1 , cf. Refs. [1,3]). We can also understand this condensation as a two step process: $D(D_4) \rightarrow D(\mathbb{Z}_2 \times \mathbb{Z}_2) \rightarrow D(\mathbb{Z}_2)$. Condensing $1c$ generates the toric code squared $D(\mathbb{Z}_2 \times \mathbb{Z}_2)$, which splits the $4a$ anyon into two Abelian anyons, the second step condenses one of the split $4a$ anyon to yield the toric code order. As α increases, the correlation length also increases (Fig. 4) but the topological order remain the same up to the phase transition.

For $\alpha = 1.4$, we find the condensation pattern

$$\begin{aligned} 1a + 2a + 4a &\rightarrow \hat{1}, \\ 1c + 2c + 4a &\rightarrow \hat{e}, \\ 3a + 5a &\rightarrow \hat{m}, \\ 3c + 5b &\rightarrow \hat{f}. \end{aligned}$$

Again, this phase has toric code topological order, but with a different condensation pattern, and thus inequivalent to the toric code found in the small α phase. Consequently, a phase transition must occur at some intermediate α (which we found numerically at $\alpha \approx 1$) if we are to preserve the D_4 symmetry of the PEPS. Note that the two condensation patterns above are exchanged if we choose to apply $\Pi(\alpha)$, Eq. (5), in the dual basis. Finally, for $\alpha = 3$, we find that anyons $1a, 1c, 2a, 2c, 4a$ have condensed into the vacuum [31], while all other anyons

have become confined; we are thus left with a trivial phase, as expected.

We have applied the same analysis also to the α -interpolation for the $\text{SYM}_{1 \times 1}$ model described in Eq. (6). For the small α phase, we can again consider $\alpha = 0$ and find a toric code with the same condensation pattern as before for $\alpha = 1.4$ (since we chose to symmetrize in the dual basis). For the large α regime, however, we cannot reliably extract the scaling of the λ_{N_0} due to the large correlation length. In order to identify the condensation pattern, we therefore choose an alternative approach: We consider an infinite plane and compute the overlap of different anyons (with a semi-infinite string attached to them), using an iMPS ansatz, cf. Ref. [18]. Here a non-Abelian anyon is described by a semi-infinite string of U_g with $g \in C_n$, terminated by an object R_{α_m} which transforms like an irrep α_m of $N[g]$; in order to account for the symmetry breaking in the boundary MPS [18,19], we additionally need to symmetrize the iMPS over the group action, since the group is non-Abelian. In order to not have to worry about the precise choice for R_α , and in order to reduce computational effort, we choose to rather compute the boundary conditions imposed on an arbitrary endpoint $R_\alpha \otimes \bar{R}_\beta$ in the overlap, and subsequently project it onto all possible irrep sectors (α, β) ; details of the method will be presented elsewhere. This way, we find that all anyons describe well-normalized and orthogonal excitations, suggesting that the large α regime corresponds to the full $D(D_4)$ phase.

-
- [1] F. A. Bais and J. K. Slingerland, *Phys. Rev. B* **79**, 045316 (2009).
 - [2] I. S. Eliëns, J. C. Romers, and F. A. Bais, *Phys. Rev. B* **90**, 195130 (2014).
 - [3] T. Neupert, H. He, C. von Keyserlingk, G. Sierra, and B. A. Bernevig, *Phys. Rev. B* **93**, 115103 (2016).
 - [4] N. Read and E. Rezayi, *Phys. Rev. B* **59**, 8084 (1999).
 - [5] A. Cappelli, L. S. Georgiev, and I. T. Todorov, *Nucl. Phys. B* **599**, 499 (2001).
 - [6] A. Kitaev, *Ann. Phys.* **303**, 2 (2003).
 - [7] B. Paredes, *Phys. Rev. B* **86**, 155122 (2012).
 - [8] B. Paredes, *arXiv:1402.3567*.
 - [9] F. Verstraete and J. I. Cirac, *Phys. Rev. A* **70**, 060302(R) (2004).
 - [10] F. Verstraete, M. M. Wolf, D. Perez-Garcia, and J. I. Cirac, *Phys. Rev. Lett.* **96**, 220601 (2006).
 - [11] N. Schuch, I. Cirac, and D. Pérez-García, *Ann. Phys.* **325**, 2153 (2010).
 - [12] M. A. Levin and X.-G. Wen, *Phys. Rev. B* **71**, 045110 (2005).
 - [13] O. Buerschaper, M. Aguado, and G. Vidal, *Phys. Rev. B* **79**, 085119 (2009).
 - [14] Z.-C. Gu, M. Levin, B. Swingle, and X.-G. Wen, *Phys. Rev. B* **79**, 085118 (2009).
 - [15] M. B. Sahinoglu, D. Williamson, N. Bultinck, M. Marien, J. Haegeman, N. Schuch, and F. Verstraete, *arXiv:1409.2150*.
 - [16] N. Bultinck, M. Mariën, D. J. Williamson, M. B. Şahinoğlu, J. Haegeman, and F. Verstraete, *arXiv:1511.08090*.
 - [17] N. Schuch, D. Poilblanc, J. I. Cirac, and D. Perez-Garcia, *Phys. Rev. Lett.* **111**, 090501 (2013).
 - [18] J. Haegeman, V. Zauner, N. Schuch, and F. Verstraete, *Nat. Commun.* **6**, 8284 (2015).
 - [19] K. Duivenvoorden, M. Iqbal, J. Haegeman, F. Verstraete, and N. Schuch (unpublished).
 - [20] N. Schuch, D. Poilblanc, J. I. Cirac, and D. Pérez-García, *Phys. Rev. B* **86**, 115108 (2012).
 - [21] N. Schuch, D. Perez-Garcia, and I. Cirac, *Phys. Rev. B* **84**, 165139 (2011).
 - [22] Note that the converse is not true: There can be tensors of the form Eq. (1) where the irrep weights in U_g are very far from the regular representation, but which nevertheless are in the $D(G)$ phase; this is related to the fact that missing irreps can be obtained by blocking (i.e., as irreps of $U_g \otimes U_g$). For instance, this is the case for the model obtained from the $D(D_4)$ model by removing the trivial irrep from the regular representation.
 - [23] C. Repellin, T. Neupert, B. A. Bernevig, and N. Regnault, *Phys. Rev. B* **92**, 115128 (2015).
 - [24] C. Fernández-González, N. Schuch, M. M. Wolf, J. I. Cirac, and D. Pérez-García, *Phys. Rev. Lett.* **109**, 260401 (2012).
 - [25] C. Fernández-González, N. Schuch, M. M. Wolf, J. I. Cirac, and D. Pérez-García, *Commun. Math. Phys.* **333**, 299 (2015).
 - [26] H. Bombin, *Phys. Rev. Lett.* **105**, 030403 (2010).
 - [27] A. Kitaev and L. Kong, *Commun. Math. Phys.* **313**, 351 (2012).
 - [28] M. Barkeshli, C.-M. Jian, and X.-L. Qi, *Phys. Rev. B* **87**, 045130 (2013).

- [29] M. Barkeshli and X.-G. Wen, [Phys. Rev. B **81**, 045323 \(2010\)](#).
- [30] Note that the largest eigenvalue of the transfer operator for the normalization $\langle \psi_{4a} | \psi_{4a} \rangle$ of the non-Abelian anyon $4a$ is degenerate, which allows it to have nonzero overlap with more than one sector (while without such a degeneracy, i.e., for Abelian anyons, the normalized overlap must always be zero or one).
- [31] The exact condensation pattern is given by $1a + 1c + 2a + 2c + 4a + 4a \rightarrow \hat{1}$, with $4a$ having twice the weight as compared to the other anyons.